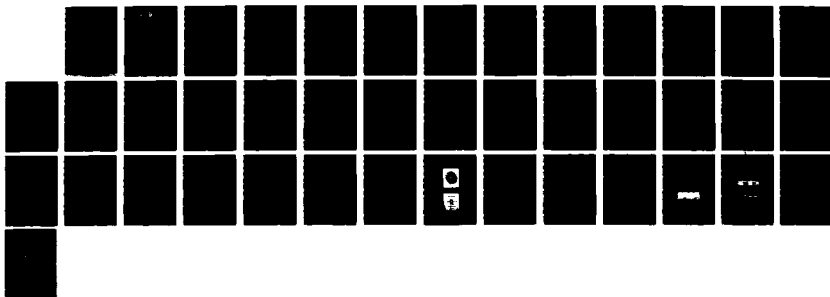SOLUBLE POLYSILANE DERIVATIVES: CHEMISTRY AND
SPECTROSCOPY(U) IBM ALMADEN RESEARCH CENTER SAN JOSE CA
R D MILLER ET AL 13 NOV 87 TR-14 N00014-85-C-0056
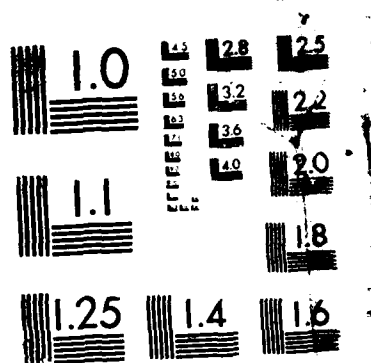
F/G 7/6

NL

MICROCOPY RESOLUTION TEST CHART
NATIONAL BUREAU OF STANDARDS 1963-A

AD-A187 889

DTIC FILE COPY

REPORT DOCUMENTATION PAGE

1a. REPORT SECURITY CLASSIFICATION Unclassified	1b. RESTRICTIVE MARKINGS
2a. SECURITY CLASSIFICATION AUTHORITY	3. DISTRIBUTION/AVAILABILITY OF REPORT
2b. DECLASSIFICATION / DOWNGRADING SCHEDULE	Approved for public release Distribution Unlimited

DEC 0 4 1987

4. PERFORMING ORGANIZATION REPORT NUMBER(S) Technical Report No. 14	5. MONITORING ORGANIZATION REPORT NUMBER(S)

6a. NAME OF PERFORMING ORGANIZATION IBM Research Division Almaden Research Center	6b. OFFICE SYMBOL (If applicable)	7a. NAME OF MONITORING ORGANIZATION ONR
6c. ADDRESS (City, State, and ZIP Code) 650 Harry Road San Jose, CA 95120-6099		7b ADDRESS (City, State, and ZIP Code) Office of Naval Research Chemistry Arlington, VA 22219
8a. NAME OF FUNDING/SPONSORING ORGANIZATION ONR (Chemistry)	8b. OFFICE SYMBOL (If applicable)	9. PROCUREMENT INSTRUMENT IDENTIFICATION NUMBER

8c. ADDRESS (City, State, and ZIP Code) 800 N. Quincy Avenue Arlington, VA 22217	10 SOURCE OF FUNDING NUMBERS			
	PROGRAM ELEMENT NO N0014-85- C-0056	PROJECT NO	TASK NO 631-850	WORK UNIT ACCESSION NO

11. TITLE (Include Security Classification)

Soluble Polysilane Derivatives: Chemistry and Spectroscopy

12. PERSONAL AUTHOR(S) R.D. Miller, J.F. Rabolt, R. Sooriyakumaran, W. Fleming, G.N. Fickes, B.L. Farmer, H. Kuzmany

13a. TYPE OF REPORT Publication	13b. TIME COVERED FROM _____ TO _____	14 DATE OF REPORT (Year, Month, Day) 87-11-13	15 PAGE COUNT 17

16. SUPPLEMENTARY NOTATION
Accepted for publication in ACS Symposium Series, Symposium on Inorganic and Organometallic Polymers, Denver Co.

17.	COSATI CODES		18. SUBJECT TERMS (Continue on reverse if necessary and identify by block number)
FIELD	GROUP	SUB-GROUP	Soluble polysilanes, structure, thermochromism, polymer
			morphology

19. ABSTRACT (Continue on reverse if necessary and identify by block number)

Polysilanes represent an interesting class of radiation sensitive polymers for which new applications have been discovered. Even though the polymer backbone is composed only of silicon-silicon single bonds, all high molecular weight polysilanes absorb strongly in the UV. The position of this absorption depends not only on the nature of the substituents, but also on the conformation of the backbone. In this regard, materials where the polymer backbone is locked into a planar zigzag conformation absorb at much longer wavelengths than comparable materials where the backbone is either disordered or nonplanar (e.g., helical). A planar zigzag backbone is often observed for symmetrically substituted derivatives in the solid state when there are also significant intermolecular interactions such as side chain crystallization. These materials are strongly thermochromic. We will discuss the thermochromism exhibited by a number of polysilanes in the solid state. Polysilane derivatives are also quite
(continued on back)

20. DISTRIBUTION/AVAILABILITY OF ABSTRACT ☐ UNCLASSIFIED/UNLIMITED ☐ SAME AS RPT. ☐ DTIC USERS	21. ABSTRACT SECURITY CLASSIFICATION
22a NAME OF RESPONSIBLE INDIVIDUAL	22b. TELEPHONE (Include Area Code)	22c. OFFICE SYMBOL

DD FORM 1473, 84 MAR

83 APR edition may be used until exhausted
All other editions are obsolete.

SECURITY CLASSIFICATION OF THIS PAGE

19. ABSTRACT (cont.)

sensitive to light and ionizing radiation. The predominant process is chain scission leading to the production of lower molecular weight fragments. Certain applications which are dependent on this radiation sensitivity are described.

"SOLUBLE POLYSILANE DERIVATIVES: CHEMISTRY AND SPECTROSCOPY:

by
R.D. Miller, J.F. Rabolt, R. Sooryakumaran, W. Fleming, G.N. Fickes,
B.L. Farmer, H. Kuzmany

IBM Almaden Research Laboratory
650 Harry Road
San Jose, CA 95120-6099
November 13, 1987

SOLUBLE POLYSILANE DERIVATIVES: CHEMISTRY AND SPECTROSCOPY

R. D. Miller
J. F. Rabolt
R. Sooriyakumaran
W. Fleming

IBM Research
Almaden Research Center
650 Harry Road
San Jose, California 95120-6099

G. N. Fickes

Department of Chemistry
University of Nevada
Reno, Nevada

B. L. Farmer

Mechanical and Materials Engineering
Washington State University
Pullman, Washington

H. Kuzmany

Institut of Festkorperphysik
University of Vienna
Vienna, Austria

ABSTRACT: Polysilanes represent an interesting class of radiation sensitive polymers for which new applications have been discovered. Even though the polymer backbone is composed only of silicon-silicon single bonds, all high molecular weight polysilanes absorb strongly in the UV. The position of this absorption depends not only on the nature of the substituents, but also on the conformation of the backbone. In this regard, materials where the polymer backbone is locked into a planar zigzag conformation absorb at much longer wavelengths than comparable materials where the backbone is either disordered or nonplanar (e.g., helical). A planar zigzag backbone is often observed for symmetrically substituted derivatives in the solid state when there are also significant intermolecular interactions such as side chain crystallization. These materials are strongly thermochromic. We will discuss the thermochromism exhibited by a number of polysilanes in the solid state. Polysilane derivatives are also quite sensitive to light and ionizing radiation. The predominant process is chain scission leading to the production of lower molecular weight fragments. Certain applications which are dependent on this radiation sensitivity are described.

(M87314S)

Polysilane derivatives, i.e., polymers containing only silicon in the backbone, are attracting considerable attention as a new class of radiation sensitive polymers with interesting spectroscopic properties (1). The first diaryl substituted polymers were probably first synthesized over 60 years ago by Kipping (2). In 1949, Burkhard (3) reported the preparation of the simplest substituted derivative poly(dimethylsilane). These early materials attracted relatively little scientific interest because of their intractable nature until the pioneering work of Yajima, who showed that poly(dimethylsilane) could be converted through a series of pyrolytic steps into β-SiC fibers with very high tensile strengths (4-7). Around the same time, a number of workers reported the preparation of a soluble homopolymer (8) and some soluble copolymers (9-10). The preparation of soluble derivatives restimulated interest in substituted silane polymers and, as a result, a number of new applications for high molecular weight polysilane derivatives have recently appeared. In this regard, they have been investigated as oxygen insensitive initiators for vinyl polymerization (11) and as a new class of polymeric photoconductors exhibiting high hole mobilities (12-14). The discovery that polysilane derivatives were radiation sensitive, coupled with their stability in oxygen plasmas, has also led to a number of microlithographic applications (15-19).

Synthesis

High molecular weight, linear, substituted silane polymers are usually prepared by a Wurtz type coupling of the corresponding dichlorosilanes initiated by sodium dispersed in an aromatic or hydrocarbon solvent (1,15,23). Recently, lower molecular weight materials have been prepared from monosubstituted silanes using a variety of titanium containing catalysts (20,21). We have prepared a large number of soluble polysilanes by the modified Wurtz coupling (23). The mechanism of polymer formation is not known with certainty, but it appears to be surface initiated, since the use of soluble aromatic radical anions does not lead to the production of high polymer. Recently, some evidence has been presented to support the involvement of radicals in the polymerization process (22).

$$R^1R^2SiCl_2 + Na \xrightarrow{\Delta} \left(\begin{array}{c} R^1 \\ | \\ -Si- \\ | \\ R^2 \end{array} \right)_n + 2NaCl$$
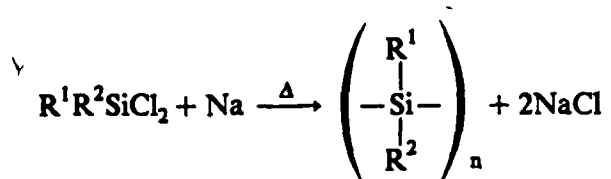
Our initial studies (23) were performed in toluene, and Table I shows the results from the polymerization of a number of representative monomers. The data reported in Table I are for "direct" addition of the monomer to the sodium dispersion. Inverse addition often leads to higher molecular weights, although the overall polymer yields are usually lower (15,23). The results in Table I show that, under these reaction conditions, a bimodal molecular molecular weight distribution is normally obtained. Furthermore, it is obvious that the crude polymer yields drop precipitously as the steric hindrance in the monomer increases.

In an effort to improve the yield of high polymer, a solvent study was conducted using a typical sterically hindered monomer dichloro-di-n-hexylsilane, and the results are shown in Table II. The use of as little as 5% by volume of diglyme in toluene led to a 6-7 fold increase in the yield of polymer. As the proportion of diglyme cosolvent decreased, the fraction of high molecular weight material in the isolated polymer increased. This polymerization can be also conducted around room temperature by using ultrasound activation both during the generation of the dispersion (24) and during the monomer addition. Interestingly, the characteristic blue color of the reaction mixture was not observed during the addition of monomer to the dispersion in pure xylene, but appeared soon after some diglyme cosolvent was added, with an attending large increase in the viscosity of the reaction mixture. The use of diglyme to improve the yield of high polymer is not limited to dichloro-di-n-hexylsilane and we have achieved significant improvements with a number of other dialkyl substituted monomers. Our preliminary studies indicate that there is usually little advantage in the use of polyether cosolvents for the polymerization of aryl substituted monomers unless the aryl ring contains a polar group such as an alkoxy substituent. Initially, it was felt that the role of the polyether solvent was cation complexation, thus promoting anionic

propagation (15). However, the use of varying amounts of the specific sodium ion complexing agent, 15-crown-5, in the polymerization of dichloro-di-n-hexylsilane failed to significantly improve the polymerization yield and led to low molecular weight materials (entries 6 and 7). Furthermore, the addition of 16% by volume of the nonpolar solvent heptane to the toluene also resulted in a good yield of high molecular weight material. These results imply that specific cation complexation probably does not play a significant role in the polymerization process and suggest instead that there is a significant bulk solvent effect for this particular example.

Spectral Properties and Polymer Morphology

One of the most intriguing properties of catenated silane derivatives is their unusual electronic spectra (25). The observation that low molecular weight silicon catenates absorb strongly in the UV was first reported by Gilman (26,27) and has been extensively studied (25). In this regard, the high molecular weight, substituted silane polymers all absorb strongly in the UV-visible region. This is an unusual feature for a polymer containing only sigma bonds in the backbone framework and differs markedly from comparable carbon backbone analogs. Earlier theoretical studies successfully treated this phenomenon using a linear combination of bond orbitals model (LCBO) (25). These predictions have been confirmed more recently using more sophisticated theoretical approaches (28-32).

Our initial spectroscopic studies on unsymmetrically substituted, atatic polysilanes derivatives resulted in a number of preliminary conclusions (33). We found that both the λ_{max} and the ϵ/Si-Si bond depended somewhat on the molecular weight, increasing rapidly at first with increased catenation and finally approaching limiting values for high molecular weight materials (33). These limiting values seem to be reached around a degree of polymerization of 40-50. Subsequent substituent studies at ambient temperatures suggested that the alkyl derivatives absorb from 305-325 nm with those polymers containing sterically demanding substituents being red shifted to longer wavelengths. The effect of the steric bulk of substituents on the absorption spectra of

alkyl substituted polymers has also been reported by other workers (19). Those polymers containing aryl substituents directly bonded to the silicon backbone are usually red shifted to longer wavelengths ($\lambda_{max} \sim$ 335-350 nm). This shift, which has been previously documented for short silicon catenates (34), was suggested to result from interactions between the σ and σ^* levels of the silicon backbone and the π and π^* states of the aromatic moiety (25). It has recently been predicted from theoretical studies, that the extent of this perturbation should also be dependent on the geometric orientation of the aromatic substituent relative to the silicon backbone (31).

Recently, variable temperature studies on certain polysilane derivatives both in solution and in the solid state indicate that the nature of the substituent effects is more complex than first indicated. This is shown dramatically in Figure 1. The absorption spectrum of poly(di-n-hexylsilane)(PDHS) in solution is not unusual and shows a broad featureless long wavelength maximum around 316 nm. The spectral properties of films of PDHS were, however, quite unexpected (35). Figure 1 shows that a spectrum of PDHS run immediately after baking at 100°C to remove solvent resembles that taken in solution except for the anticipated broadening. However, upon standing at room temperature, the peak at 316 nm is gradually replaced by a sharper band around 372 nm. This process is completely thermally reversible upon heating above 50°C and recooling. DSC analysis of the sample revealed a strong endotherm (ΔH = 4.0 Kcal/mol) around 42°C. The corresponding cooling exotherm was observed around 20°C, the exact position being somewhat dependent on the cooling rate. This thermal behavior is reminiscent of that observed for a number of isotactic polyethylene derivatives substituted with long chain alkyl substituents (36-39). For the polyolefins, the thermal transition has been attributed to the crystallization of the hydrocarbon side chains into a regular matrix. However, the significant changes in the electronic spectrum of PDHS at the transition temperature suggest that the nature of the backbone chromophore is also being altered during the process.

IR and Raman spectroscopic studies on films and powders of PDHS indicate that the hexyl side chains are crystallizing into a hydrocarbon type matrix (40). This is indicated by the presence of a number of sharp characteristic alkane bands which become dramatically broadened above the transition temperature. Similar changes are observed for n-hexane below and above the melting point. CPMAS ^{29}Si NMR studies on PDHS also show that the rotational freedom of the side chains increases markedly above the transition temperature (41,42). All of the spectral evidence supports the suggestion that the side chains of PDHS are crystallizing below 42°C and that side chain melting is to a large extent associated with the observed thermal endotherm.

While it was somewhat unexpected that conformational changes in a sigma bonded backbone would produce such a dramatic effect on the absorption spectrum, this is not totally without precedent in silicon catenates. In this regard, Bock et al. (43) have suggested that conformational equilibration in short chain silicon catenates is responsible for the complexity of their photoelectron spectra. Recent theoretical studies (32) on larger silicon catenates have not only confirmed the dependence of the electronic properties on the backbone conformation, but have also suggested that the all trans, planar zigzag conformation should absorb at significantly longer wavelengths than the gauche conformations. This data strongly suggests that the red shift observed for PDHS upon cooling below 42°C is associated with a backbone conformational change initiated by side chain crystallization and, furthermore, that the backbone below the transition temperature is trans or planar zigzag. This hypothesis was confirmed by wide-angle X-ray diffraction and Raman studies on stretch-aligned films of PDHS (44,45). At room temperature, WAXD analysis yielded over 40 distinct reflections from 5-45°, 20 of which were indexed (44). The layer line spacing of 4.07Å and the appearance of a strong meridional spot on the third layer line in the inclined film confirms the planar zigzag nature of the polymer backbone. At 60°C, a single sharp reflection remains on the equator (13.5Å) corresponding to the silicon-silicon interchain distance. The maintenance of this strong reflection for long periods of time above the transition

temperature suggests that all order is not lost, even though the side chain melting transition is associated with a conformational disordering of the silicon backbone resulting in a 60 nm blue shift in the absorption spectrum (44).

This thermochromic behavior is not limited to PDHS itself but extends to other symmetrical derivatives with longer n-alkyl chains (38,42). The thermochromism of the higher homologs is, however, frequently more complex than that observed for PDHS. Although all of the higher homologs examined (up to C_{14}) show side chain crystallization as evidenced by their IR and Raman spectra and the observation of a reversible endotherm (ΔH = 4.5-8.0 Kcal/mol) by DSC (Tm ~ 43-55°C), the nature of the spectral shifts displayed by these materials is variable. For example, although the heptyl and octyl derivatives behave almost identically to PDHS, the decyl derivative is more complex (see Table III). In the latter case, there exist at least two phases, each observable by DSC analysis. The low temperature phase, characterized by a thermal transition around 31°C, has a UV absorption maximum around 350 nm. Another phase, with a transition near 45°C, absorbs at much longer wavelengths, around 380 nm. The previous analysis would suggest that the phase which absorbs at the longer wavelength is more likely to contain the silicon backbone in a planar zigzag conformation. The tetradecyl derivative apparently forms a single phase (Tm ~ 54°C) and absorbs at 347 nm. The nature of the backbone conformation(s) for those materials absorbing around 350 nm has not yet been determined but it is most probably not planar zigzag. Apparently, the longer alkyl chains can still crystallize without enforcing a planar zigzag conformation of the backbone. A less likely alternative than a nonplanar backbone for those materials which absorb around 350 nm would be a planar zigzag backbone conformation where the silicon-silicon valence angles are significantly distorted fiom those values observed for PDHS by the size of the substituents and/or the mode in which they crystallize. Due to the nature of the orbital interactions in sigma bonded systems, the HOMO-LUMO excitation energy will be quite sensitive to changes in these valence angles even more so than to changes in the silicon-silicon bond lengths (31). On the

basis of the above information, we submit that significant intermolecular interactions in the solid state (e.g., side chain crystallization) are a necessary but not always sufficient condition to force a planar zigzag conformation of the silicon backbone and in their absence the backbone either disorders or adopts alternative nonplanar conformations.

If the alkyl substituent in a dialkyl substituted polysilane is either too short or is branched, it cannot pack properly to allow side chain crystallization, and hence, one would expect very different, properties from PDHS and its higher homologs. In order to study this possibility, we synthesized and characterized the di-n-butyl (PDBS), di-n-pentyl (PDPS) and di-5-methylhexyl polymers (PDMHS). A film of the branched chain 5-methylhexyl polymer absorbed at 315 nm and the position of this maximum was relatively insensitive to temperature. Likewise, no thermal transition was observed in the region where the side chain melting transition was seen for PDHS and its higher homologs.

The thermal and optical characteristics of PDBS and PDPS are very similar and the latter will be used for illustrative purposes. The λ_{max} of PDNPS both in solution and as a solid film occurs around 314 nm. The absorption maximum of the film is unusually narrow relative to other polysilane samples with a full width at half height of 22 nm (see Figure 2). Cooling to $-60°C$ has little effect except for the appearance of a small, broad shoulder at 340 nm. Heating, however, results in a dramatic change which is shown in Figure 2. Above 75°C, the absorption broadens markedly ($w_{1/2} = 58$ nm) but the λ_{max} remains essentially unchanged. DSC analysis reveals the presence of a weak reversible endotherm ($\Delta H = 0.45$ Kcal/mol) at 74°C. It is significant that the nature of this transition is very different from that observed in PDHS (42°C, $\Delta H = 5$ Kcal/mol). In the latter case, the transition has been attributed to a combination of side chain melting and the subsequent disordering of the planar zigzag backbone. The other spectroscopic data for PDPS (46) is also very different from that described for PDHS. Figure 3 shows a comparison of the Raman spectra for the two materials. Particularly obvious is the absence of the strong characteristic band at

689 cm^{-1} for PDHS which had previously been assigned as a silicon-carbon vibration in the rigidly locked planar zigzag conformation. The CPMAS ^{29}Si NMR spectra of PDHS and PDHS are also markedly different (Figure 4). In particular, it should be noted that the silicon signal for PDPS, which is relatively narrow, is significantly upfield from that of PDHS below the transition temperature. It is interesting that at 87°C, which is above the respective phase transition temperatures of each polymer, the silicon signal of each sample becomes a narrow, time averaged resonance around -23.5 ppm relative to TMS. All of the comparative spectral data suggests that PDPS exists in a regular structure in the solid state below 74°C which is, however, different from the planar zigzag form of PDHS.

We have successfully stretch-aligned samples of PDPS, and the film diffraction pattern is compared with that of PDHS in Figure 5. From an analysis of this data, it is obvious that the backbone of PDPS is not planar zigzag but is, in fact, helical (44). The diffraction data suggests that PDPS exists as a 7/3 helix in the solid state where each silicon-silicon bond is advanced by approximately 30° from the planar zigzag conformation (Figure 6). A stable helical conformation for polysilane derivatives containing bulky substituents in the absence of intermolecular interactions is also consistent with recent calculations (47). The data shows for the first time that significant deviation from the trans backbone conformation, even in a regular structure, results in a large blue shift (~60 nm) in the UV absorption spectrum. On the basis of the results described, it now seems that the absorption spectra normally observed for alkyl polysilane derivatives ($\lambda_{max} \sim$ 305-325 nm) may arise either from conformational disorder in the backbone or from systematic deviations from the planar zigzag conformation even in regular structures and do not represent the intrinsic limiting absorption for an alkyl substituted polysilane chain.

In a continuing study of substituent effects on the spectra of polysilane derivatives, we have succeeded in the preparation of the first soluble poly(diarylsilane) homopolymers. Materials of this type have traditionally proved to be insoluble and

intractable. Very recently, West and co-workers have reported the preparation of some soluble copolymers which contain diphenylsilylene units (48,49).

The soluble substituted diaryl homopolymers were prepared by the condensation of the respective substituted silyl dichlorides with sodium (48). The yields of these polymerizations were predictably low (~10%) as expected based on previous studies on sterically hindered monomers.

The most extraordinary feature of the soluble poly(diarylsilanes) is their remarkable absorption spectra. In this regard, they absorb around 400 nm, making them by far the most red shifted of any polysilane derivatives studied thus far. Some representative spectral data is shown in Table IV. Included in the table for comparison are data for poly(methylphenylsilane) and a random copolymer containing diphenylsilylene units. The long wavelength absorption band of the diaryl polysilanes in solution is exceptionally narrow (11-16 nm) for a polymeric material containing a backbone chromophore. Surprisingly, there is very little difference in the spectra recorded either in dilute solution or as films except for some broadening in the solid sample.

The origin of the large spectral red shifts observed for these materials is under active investigation. At this point, however, they seem much too large to be attributed to typical electronic substituent effects alone. In this regard, poly(phenylmethylsilane) is red shifted from typical atatic dialkyl derivatives by ~25-30 nm. This shift has been attributed to the electronic interaction of the substituent π and π^* orbitals with the backbone σ and σ^* levels. Even if the addition of a second aromatic group contributed similarly to the spectrum, which is highly unlikely based on the study of model compounds (34,51,52), the materials would be expected to absorb around 360-365 nm. In this regard, the random 1:1 copolymer prepared from the condensation of diphenyl silyl dichloride with hexylmethylsilyl dichloride absorbs around 350 nm. It therefore seems likely that the explanation of the unexpectedly large red shifts observed for the

soluble diaryl polysilane homopolymers requires something other than a simple electronic substituent effect.

One intriguing, albeit tentative, explanation is that these spectral shifts also are conformational in origin. It is interesting that the magnitude of the observed shifts (50-60 nm) relative to poly(methylphenylsilane) is very similar to that observed for the poly(di-n-alkylsilanes) when they undergo a change from a disordered backbone to a regular planar zigzag arrangement (35,40). Although the close correspondence between the magnitude of the spectral shifts observed in each system may be fortuitous, it does raise the possibility that the diaryl derivatives adopt an extended planar zigzag conformation even in solution without the intervention of significant intermolecular interactions. This argument does not necessarily require that these polymers must exist exclusively as rigid rods, but the position of the long wavelength transition would argue that all-trans runs of significant length be present in solution. While the suggestion that the origin of the red shifts observed for the soluble diaryl polysilanes is conformational is intriguing, the final answer must await further structural and spectroscopic studies both in solution and in the solid state.

Photochemistry

Since both the λ_{max} and the ϵ_{SiSi} depend on the molecular weight up to a degree of polymerization of 40-50 (31), any process which induces significant chain scission should result in bleaching of the initial absorbance. Conversely, crosslinking processes which maintain or increase the molecular weight of the polymer should lead to very little bleaching. All of the polysilane derivatives which we have examined thus far undergo significant bleaching upon irradiation (15) both in solution and as films (see Figure 7 for a representative example) albeit the rate varies somewhat with structure. In general, the alkyl substituted materials bleach more rapidly than the aryl derivatives in the solid state and among the former those with bulky substituents usually bleach most rapidly. GPC examination of the polymer solutions after irradiation show that the molecular weight is continuously reduced. Alkyl derivatives such as poly(methyldodecylsilane) cleanly

scission and the molecular weight decreases regularly upon irradiation. The GPC traces of such materials show no high molecular weight tail. On the other hand, aromatic polysilane derivatives such as poly(phenylmethylsilane) are not cleanly converted to lower molecular weight materials upon irradiation and the GPC analysis of these irradiated materials clearly show the presence of a higher molecular tail suggesting that concurrent crosslinking is occurring (33). Materials such as PDHS which absorb at ~370 nm after standing for some time to allow side chain crystallization to orient the backbone into a planar zigzag configuration can also be bleached upon irradiation at 365 nm with the formation of lower molecular weight fragments. The soluble poly(diarylsilanes) are bleached very readily upon irradiation at 404 nm in solution, but much more slowly in the solid state. One possible explanation for this latter observation is that the absence of readily available α-hydrogens for disproportionation of the silyl chain radicals produced by photoscission promotes rapid recombination resulting in chain repair (vide infra).

The quantum yields for both chain scission (Φ_s) and crosslinking (Φ_x) can be estimated from plots of $1/\overline{M}n$ and $1/\overline{M}_w$ versus the absorbed dose in photochemical and other radiation induced processes (51,52). In general, the photochemical quantum yields for scission are quite high for the polysilane derivatives in solution and vary from ~0.5-1.0. The alkyl substituted derivatives show little tendency to crosslink during irradiation ($\Phi_x = 0$-0.08). On the other hand, aromatic materials such as poly(methylphenylsilane) and related derivatives are more prone to crosslinking ($\Phi_x \sim 0.12$-0.18), although chain scission is still the predominate process ($\Phi_s/\Phi_x \sim 5$-7). One particularly clear trend is that the efficiency for both scission and crosslinking is significantly reduced in the solid state relative to solution by as much as a factor of 50-100.
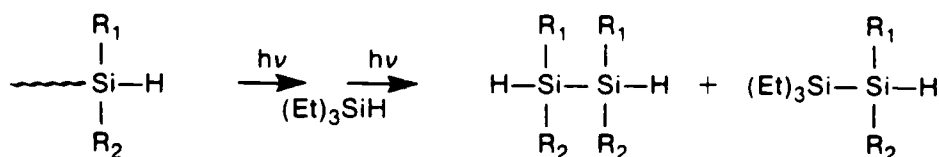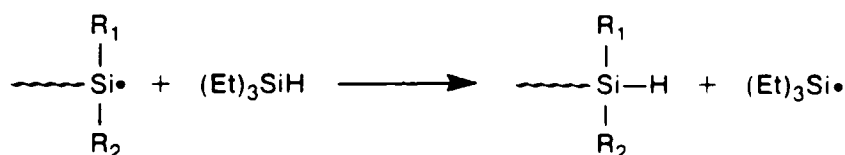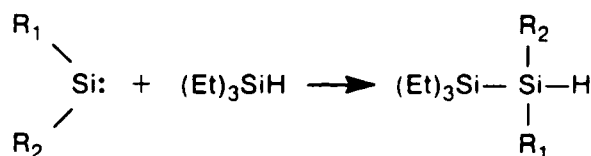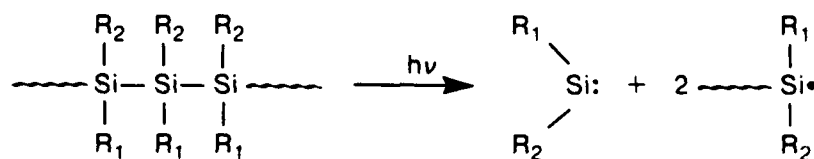
The presence of air is not necessary for photobleaching, although in vacuum, the efficiency depends somewhat on the nature of the substituents. This suggested that the polysilanes might have some potential as positive functioning e-beam resists (vide infra).

To conveniently assess their sensitivity toward ionizing radiation, samples of poly(p-t-butylphenyl methylsilane) poly(di-n-butylsilane) and poly(di-n-pentylsilane) were placed in Pyrex tubes, sealed under vacuum and subjected to γ-radiolysis from a ^{60}Co source. After irradiation, the samples were opened and analyzed by GPC. In each case, polymer scission was the predominate pathway and the G(s) values varied from ~0.14 to 0.4. Under the same conditions, the G(s) value of PMMA was calculated to be 1.2. The alkyl polysilane derivatives were ~3 times more sensitive than the aromatic polymer. The observed crosslinking was relatively minor in each case and the ratios of G(s)/G(x) were all greater than 20.

Previous photochemical studies on acyclic silane oligomers have shown that both silyl radicals and substituted silylenes are intermediates in the irradiation (55,56). It has recently been suggested that monomeric silylene species are also major gas phase intermediates in the laser induced photoablation of a number of alkyl substituted copolymers (19). Accordingly, we have exhaustively irradiated a number of high molecular weight polysilane derivatives at 254 nm in the presence of trapping reagents such as triethylsilane and various alcohols (57). With the former reagent, the major products were the triethylsilane adducts of the substituted silylene fragment extruded from the polymer chain. Also produced in reasonable yield were disilanes carrying the substitution pattern of the polymer chain. The disilane fragments apparently accumulate in the photolysis mixture, because they are only weakly absorbing at 254 nm. These results suggest that silylenes and silyl radicals are both generated upon exhaustive photolysis of the linear substituted silane polymers. The silanes produced by abstraction of a hydrogen atom from the trapping reagent are subjected to further chain degradation until they reach the stage where they no longer efficiently absorb the light. The results from the photolysis in alcoholic solvents were also consistent with silylenes and silyl radicals as intermediates (57). These studies lead us to postulate the mechanism shown below for the photodegration of polysilane high polymers in solution. It is not known

whether the silylenes are produced concurrently with or subsequently to the formation of the silyl chain radicals.

Mechanism

$$\underset{\underset{R_1\ R_1\ R_1}{|\ \ |\ \ |}}{\overset{\overset{R_2\ R_2\ R_2}{|\ \ |\ \ |}}{-Si-Si-Si-}} \quad \xrightarrow{h\nu} \quad \underset{R_2}{\overset{R_1}{\diagdown}} Si: \ + \ 2 \underset{R_2}{\overset{R_1}{\underset{|}{\overset{|}{-Si\bullet}}}}$$

$$\underset{R_2}{\overset{R_1}{\diagdown}} Si: \ + \ (Et)_3SiH \ \longrightarrow \ (Et)_3Si-\underset{R_1}{\overset{R_2}{\underset{|}{\overset{|}{Si}}}}-H$$

$$\underset{R_2}{\overset{R_1}{\underset{|}{\overset{|}{-Si\bullet}}}} \ + \ (Et)_3SiH \ \longrightarrow \ \underset{R_2}{\overset{R_1}{\underset{|}{\overset{|}{-Si}}}}-H \ + \ (Et)_3Si\bullet$$

$$\underset{R_2}{\overset{R_1}{\underset{|}{\overset{|}{-Si}}}}-H \ \xrightarrow[\ ]{h\nu} \xrightarrow[(Et)_3SiH]{h\nu} \ H-\underset{R_2}{\overset{R_1}{\underset{|}{\overset{|}{Si}}}}-\underset{R_2}{\overset{R_1}{\underset{|}{\overset{|}{Si}}}}-H \ + \ (Et)_3Si-\underset{R_2}{\overset{R_1}{\underset{|}{\overset{|}{Si}}}}-H$$

Polysilanes for Microlithography

The trend in microlithography is toward denser circuitry containing features with smaller lateral dimensions. Due to unavoidable chip topography, the lateral dimensions are shrinking more rapidly than the vertical with an attending increase in the feature aspect ratio (height/width). This creates numerous problems for classical single layer resist processes and has led lithographers to explore multilayer alternatives in spite of their increased processing complexity (58). A basic description of a typical single and multilayer process is shown in Figure 8. The classical single layer, wet development process requires exposure of the resist, followed by development of the pattern using appropriate solvent developer. Since wet development processes are usually isotropic,

for small features there is often loss in linewidth control and sloping nonvertical profiles may be produced. This can create problems at later stages in the process. On the right side of Figure 8 is pictured an idealized multilayer process. The wafer topography is first covered with a thick, inert planarizing polymer layer followed by a thin layer of resist. Since the resist layer can be much thinner than is acceptable in a single layer application, it can be imaged with high resolution. This pattern can be either wet developed or alternatively developed during imaging (ablative exposure) down to the planarizing layer. The problems associated with wet development in this case are ameliorated relative to the single layer because the resist layer is so thin (500Å to 0.2μ relative to $\sim 1\mu$ for a single layer). The image is then transferred through the planarizing polymer layer using a reactive oxygen plasma. This dry etch process can be made highly anisotropic so the linewidth control and feature profile is excellent.

One potential problem with the multilayer process is that the photoresist remaining after imaging must be resistant to the oxygen plasma in order to effectively mask the underlying polymer. Since oxygen plasmas are very aggressive, the best organic etch barriers are materials which form refractory oxides upon plasma treatment. This has stimulated the investigation of organometallic polymers, particularly those containing silicon (59). The polysilanes are ideal for such purposes, since they are thermally stable, soluble for coating, imagable by light and ionizing radiation and stable to oxygen etching due to the formation of a thin layer of inert SiO_2.

To date, we have exercised these materials in basically three types of multilayer lithographic applications (1) as short wavelength contrast enhancing layers, (2) as imagable O_2-RIE resistant materials in bilayer processes and (3) as radiation sensitive materials for multilayer, e-beam processes.

Contrast enhancement lithography is a clever procedure which uses a bleachable contrast enhancing layer to restore the distorted aerial image of the mask which has been blurred by diffraction effects into a sharp image at the underlying photoresist surface.

The process is too complicated to explain in detail here and the interested reader is referred to the cited literature (60,61). Suffice it to say that the large extinction coefficients of most polysilane derivatives coupled with their ready bleachability make them ideally suited for such purposes and we have demonstrated this application at 313 nm (16,18).

The use of polysilanes as imagable, oxygen plasma resistant materials in bilayer applications has been explored in great detail. Using this technique and employing wet development techniques to develop the polysilane, we have generated submicron images with vertical wall profiles as shown in Figure 9 (17,18). In addition, a variation of this procedure where the polysilane is photoablatively removed during imaging has been used to create submicron images with vertical wall profiles in an "all dry" process (i.e., one which does not require wet development of the initial image (18,62)..

Finally, the sensitivity of the polysilanes to ionizing radiation has allowed us to utilize these materials in a maskless e-beam imaging process. High resolution patterns such as shown in Figure 10 have been created by imaging a suitable polysilane derivative in a bilayer configuration. The e-beam image was wet developed and transferred by oxygen reactive ion etching.

In summary, the polysilanes comprise a new class of scientifically interesting, radiation sensitive materials for which many applications have become recently apparent. There is every reason to believe that future investigations will continue to be scientifically rewarding and result in new applications.

ACKNOWLEDGMENTS

REFERENCES

1. West, R. *J. Organomet. Chem.* 1986, *300*, 327, and references cited therein.

2. Kipping, F. S. *J. Chem. Soc.* 1924, *125*, 2291.

3. Burkhard, C. A. *J. Am. Chem. Soc.* 1949, *71*, 963.

4. Yajima, S.; Hayashi, J.; Omori, M. *Chem. Lett.* 1975, 931.

5. Yajima, S.; Okamura, K.; Hayashi, J.; *J. Chem. Lett.* 1975, 720.

6. Hasegawa, Y.; Iimura, M.; Yajima, S. *J. Mater. Sci.* 1980, *15*, 1209.

7. West, R. in "Ultrastructure Processing of Ceramics, Glasses, and Composites"; Hench, L. and Ulrich, D. C., eds.; John Wiley and Sons, Inc.: New York, 1984.

8. Trijillo, R. E. *J. Organomet. Chem.* 1980, *198*, C27.

9. Wesson, J. P.; Williams, T. C. *J. Polym. Sci., Polym. Chem. Ed.,* 1980, *180*, 959.

10. West, R.; David, L. D.; Djurovich, P. I.; Stearley, K. L.; Srinivasan, K. S. V.; Yu, H. G. *J. Am. Chem. Soc.* 1981, *103*, 7352.

11. West, R.; Wolff, A. R.; Peterson, D. J. *J. Rad. Curing* 1986, *13*, 35.

12. Kepler, R. G.; Zeigler, J. M.; Harrah, L. A.; Kurtz, S. R. *Bull. APS* 1983, *28*, 362.

13. Kepler, R. G.; Zeigler J. M.; Harrah, L. A. *Bull. APS* 1984, *29*, 504.

14. Stolka, M.; Yuh, H.-J.; McGrane, K.; Pai, D. M. *J. Polym. Sci. Part A: Polym. Chem.* 1987, *25*, 823.

15. Miller, R. D.; McKean, D. R.; Hofer, D.; Willson, C. G.; West, R.; Trefonas, III, P. T. in "Materials for Microlithography"; Thompson, L. F.; Willson, C. G.; Féchet, J. M. J., eds.; ACS Symposium Series, No. 266; American Chemical Society: Washington D.C., 1984, Chap. 3.

16. Hofer, D. C.; Miller, R. D.; Willson, C. G.; Neureuther, A. R. *Proc. of SPIE* 1984, *469*, 108.

17. Hofer, D. C.; Miller, R. D.; Willson, C. G. *Proc. of SPIE* 1984 *469*, 16.

18. Miller, R. D.; Hofer, D.; Fickes, G. N.; Willson, C. G.; Marinero, E.; Trefonas, III, P.; West, R. *Polym. Eng. Sci.* 1986, *26*, 1129.

19. Zeigler, J. M.; Harrah, L. A.; Johnson, A. W. *Proc. of SPIE* 1985, *539* 166.

20. Aitken, C. T.; Harrod, J. F.; Samuel, E. *J. Am. Chem. Soc.* 1986, *108*, 4059.

21. Aitken, C. T.; Harrod, J. F.; Samuel, E. *Can. J. Chem.* **1986**, *64*, 1677.

22. Zeigler, J. M.; Harrah, L. A.; Johnson, A. W. *Polym. Preprints* **1987**, *28*, 424.

23. Trefonas, III, P.; Djurovich, P. I.; Zhang, X.-H.; West, R.; Miller, R. D.; Hofer, D. *J. Polym. Sci., Polym. Lett. Ed.* **1983**, *21*, 819.

24. Luche, J. L.; Dupuy, C. P. *Tet. Lett.* **1984**, *25*, 753.

25. Pitt, C. G., in "Homoatomic Rings, Chains and Macromolecules of Main Group Elements"; Rheingold, A. L., ed.; Elsevier: Amsterdam, 1977, 203, and references cited therein.

26. Gilman, H.; Atwell, W. H.; Schwebke, G. L. *Chem. Ind. (London)* **1964**, 1063.

27. Gilman, H.; Atwell, W. H.; Schwebke, G. L. *J. Organometal. Chem.* **1964**, *371*.

28. Bigelow, R. W. *Organometallics* **1964**, *5*, 1502.

29. Bigelow, R. W. *Chem. Phys. Lett.* **1986**, *126*, 63.

30. Takeda, K.; Matsumoto, N.; Fukuchi, M. *Phys. Rev. B* **1984**, *30*, 5871.

31. Takeda, K.; Teramar, K. A.; Matsumoto, N. *J. Am. Chem. Soc.* **1986**, *108*, 8199.

32. Klingensmith, K. A.; Downing, J. W.; Miller, R. D.; Michl, J. *J. Am. Chem. Soc.* **1986**, *108*, 7438.

33. Trefonas, III, P.; West, R.; Miller, R. D.; Hofer, D. *J. Polym. Sci., Polym. Lett. Ed.* **1983**, *21*, 823.

34. Pitt, C. G.; Carey, R. N.; Toren, Jr., E. C. *J. Am. Chem. Soc.* **1972**, *94*, 3806.

35. Miller, R. D.; Hofer, D.; Rabolt, J.; Fickes, G. N. *J. Am. Chem. Soc.* **1985**, *107*, 2172.

36. Reding, F. P. *J. Polym. Sci.* **1956**, *21*, 547.

37. Clark, K. J.; Jones, A. T.; Sandeford, D. J. H. *Chem. Ind. (London)* **1962**, 2010.

38. Jones, A. T. *Makromol. Chem.* **1964**, *71*, 1.

39. Trafara, G.; Koch, R.; Blum, K.; Hummel, D. *Makromol. Chem.* **1976**, *177*, 1089.

40. Rabolt, J. F.; Hofer, D.; Miller, R. D.; Fickes, G. N. *Macromolecules* **1986**, *19*, 611.

41. Gobbi, G. C.; Fleming, W. W.; Sooriyakumaran, R.; Miller, R. D. *J. Am. Chem. Soc.* **1986**, *108*, 5624.

42. Schilling, F. C.; Bovey, F. A.; Lovinger, A. J.; Zeigler, J. M. *Macromolecules* 1986, *19*, 2660.

43. Bock, H.; Ensslin, W.; Fehér, F.; Freund, R. *J. Am. Chem. Soc.* 1976, *98*, 668.

44. Kuzmany, H.; Rabolt, J. F.; Farmer, B. L.; Miller, R. D. *J. Chem. Phys.* 1986, *85*, 7413.

45. Lovinger, A. J.; Schilling, F. C.; Bovey, F. A; Zeigler, J. M. *Macromolecules* 1986, *19*, 2657.

46. Miller, R. D.; Farmer, B. L.; Fleming, W.; Sooriyakumaran, R.; Rabolt, J. *J. Am. Chem. Soc.* 1987, *109*, 2509.

47. Farmer, B. L.; Rabolt, J. F.; Miler, R. D. *Macromolecules* 1987 (in press).

48. Zhang, X. H.; West, R. *J. Polym. Sci., Polym. Lett. Ed.* 1985, *23*, 479.

49. Zhang, X. H.; West, R. *J. Polym. Sci., Polym. Chem. Ed.* 1984, *22*, 159.

50. Miller, R. D.; Sooriyakumaran, R. *J. Polym. Sci., Polym. Lett. Ed.* 1987 (in press).

51. Sakurai, H. *J. Organomet. Chem.* 1980, *200*, 261.

52. Kumada, M.; Tamao, K. *Adv. Organomet. Chem.* 1968, *6*, 81.

53. Kilb, R. W. *J. Phys. Chem.* 1959, *63*, 1838.

54. Schnabel, W.; Kiwi, J. in "Aspects of Degradation and Stabilization of Polymers"; Jellinek, H. H. G., ed.; Elsevier: New York, 1978, Chap. 4.

55. Ishikawa, M.: Takaoka, T.; Kumada, M. *J. Organomet. Chem.* 1972, *42*, 333.

56. Ishikawa, M.; Kumada, M. *Adv. Organomet. Chem.* 1981, *19*, 51, and references cited therein.

57. Trefonas, III, P.; West, R.; Miller, R. D. *J. Am. Chem. Soc.* 1985, *107*, 2737.

58. Lin, B. J., in "Introduction to Microlithography"; Thompson, L. F.; Willson, C. G.; Bowden, M. G., eds.; ACS Symposium Series, No. 219, American Chemical Society: Washington D.C., 1983, Chap. 5.

59. Reichmanis, E.; Smolinsky, G.; Wilkins, Jr., C. W. *Solid State Technol.* 1985, *28(8)*, 130, and references cited therein.

60. Griffing, B. F.; West, P. R. *Polym. Eng. Sci.* 1983, *23*, 947.

61. West, P. R.; Griffing, B. F. *Proc. of SPIE* 1984, *33*, 394.

62. Marinero, E. E.; Miller, R. D. *Appl. Phys. Lett.* 1987 (in press).

FIGURE CAPTIONS

Table I. Some representative polysilanes produced in toluene using sodium in a direct addition mode.

Table II. Solvent effects on the polymerization of dichloro-di-n-hexylsilane.

Table III. Transition temperatures and absorption maxima of some di-n-alkyl polysilane films.

Table IV. UV-visible spectrosopic data for some soluble diaryl polysilanes in hexane.

Figure 1. UV spectra of poly(di-n-hexylsilane); (− • −) solution in hexane; (− − −) film immediately after baking at 100°C; (——) film upon standing 3h at 21°C.

Figure 2. Variable temperature UV spectra of a poly(di-n-pentylsilane) (PDPS) film.

Figure 3. Raman spectra of PDHS (upper) and PDPS (lower) at 21°C.

Figure 4. Variable tempreature CPMAS ^{29}Si NMR spectra of PDHS (left) and PDPS (right).

Figure 5. Room temperature, wide angle x-ray diffraction (WAXD) pictures of stretch oriented samples of PDHS (upper) and PDPS (lower).

Figure 6. Projection of the 7/3 helical conformation of PDPS onto a plane normal to the helical axis. Silicon atoms are represented by the larger filled circles, carbon atoms by the smaller.

Figure 7. The photochemical bleaching of poly(hexylmethylsilane) at 313 nm.

Figure 8. A schematic for a typical single layer (left) and a multilayer lithographic process.

Figure 9. 0.75 μm features produced in a bilyer composed of 0.2 μm poly(methylcyclohexylsilane) coated over 2.0 μm of a hardbaked Novolac-naphthoquinone-2-diazide photoresist; mid-UV projection lithography, 100 mJ/cm^2, O_2-RIE image transfer.

Figure 10. Submicron features generated by e-beam imaging of 0.14 μm of an aliphatic polysilane over 2.0 μm of hardbaked Novolac-naphthoquinone-2-diazide photoresist; 20 μC, O_2-RIE image transfer.

Polymer	Yield (%)	$\overline{M}_n \times 10^{-3}$	$\overline{M}_w \times 10^{-3}$	$\overline{M}_w/\overline{M}_n$	R
(PhMeSi)$_n$	60	107	193	1.81	0.72
(β-Phenethyl MeSi)$_n$	24	5.6	9.9	1.69	4.6
		83.2	240	2.9	
(n-PrMe)Si$_n$	32	2.5	3.1	1.2	0.27
		297	644	2.17	
(n-Hexyl MeSi)$_n$	12	7.4	13.3	1.79	2.4
		281	524	1.86	
(n-Dodecyl MeSi)$_n$	8	14.6	20.5	1.40	—
		172	483	2.81	
(cyc-Hexyl MeSi)$_n$	10	300	804	2.67	8.7
		3.2	4.5	1.40	
[(C$_6$H$_{13}$)$_2$ Si]$_n$	6	1120	1982	1.77	3.12
		1.10	1.2	1.13	
[(C$_{10}$H$_{21}$)$_2$ Si]$_n$	3	521	1693	3.2	5.3
		1.18	1.42	1.21	

Table I. Some representative polysilanes produced in toluene using sodium in a direct addition mode.

Entry	Additive in Toluene	Yield (%)	$\overline{M}_n \times 10^{-3}$	$\overline{M}_w \times 10^{-3}$	$\overline{M}_w/\overline{M}_n$	$R\left(\dfrac{\text{High Molecular wt}}{\text{Low Molecular wt}}\right)$
1	Toluene only	6	1982 1.2	1120 1.1	1.77 1.13	3.12
2	30% Diglyme	37	1073 31.7	561 13.5	1.9 2.3	1.42
3	10% Diglyme	36	1358 26.6	712 13.0	1.9 2.1	2.61
4	5% Diglyme	34	1008 22.3	539 12.6	1.87 1.79	3.41
5	25% Diglyme 75% Xylene (Ultrasound)	22	37.6	14.0	2.7	—
6	15-Crown-5 0.5 mmol/mmol Na	18	6.4	4.5	1.42	—
7	15-Crown-5 1.1 mmol/mmol Na	13	6.4	4.6	1.38	—
8	16% Heptane	27	1386 1.12	679 1.09	2.04 1.03	9.61

Table II. Solvent effects on the polymerization of dichloro-di-n-hexylsilane.

Polymer	λ shift (nm)	$T_m(°C)$
poly(di-n-hexyl silane)	317 → 374	42
poly(di-n-heptyl silane)	317 → 374	45*
poly(di-n-octyl silane)	317 → 374	43*
poly(di-n-decyl silane)	320 → 383	45
	(320 → 350)	(28)
poly(di-n-tetradecyl silane)	322 → 347	54

*measured by IR

Table III. Transition temperatures and absorption maxima of some di-n-alkyl polysilane films.

Polymer	λ_{max}	$\epsilon \times 10^{-3}/SiSi$
	390	10.2
	395	26.6
	390	16.2
	376	3.4
	397	23.3
	400	21.3
	394	18.6
$(PhMeSi)_n$	340	9.0
$-[(Ph)_2Si]_x-co-[Me\ Hexyl\ Si]_y$	350	5.5

Table IV. UV-visible spectrosopic data for some soluble diaryl polysilanes in hexane.
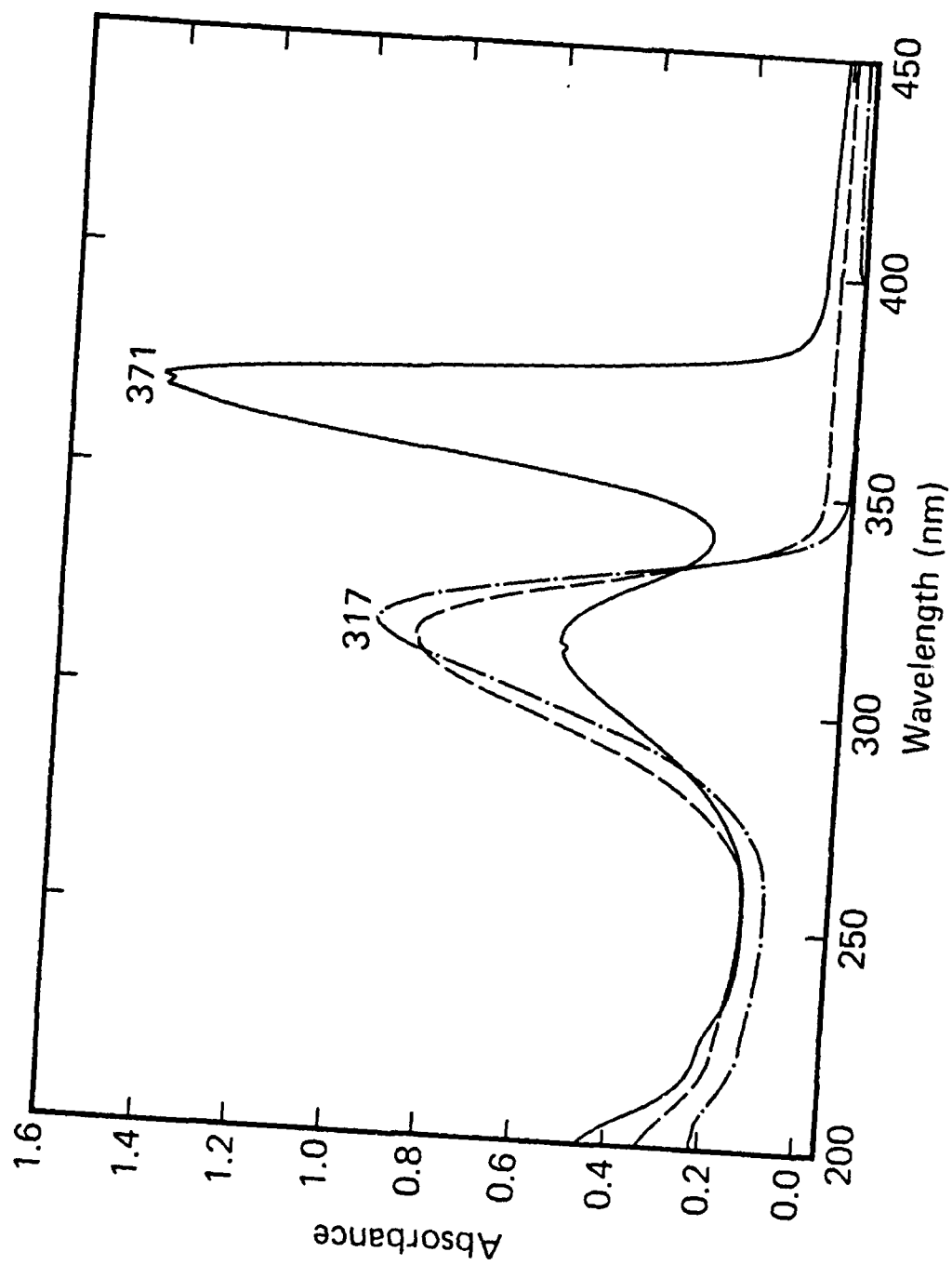
Figure 1. UV spectra of poly(di-n-hexylsilane); (— • —) solution in hexane; (— — —) film immediately after baking at 100°C; (———) film upon standing 3h at 21°C

Variable Temperature UV Spectra of Poly(di–n–pentylsilane)
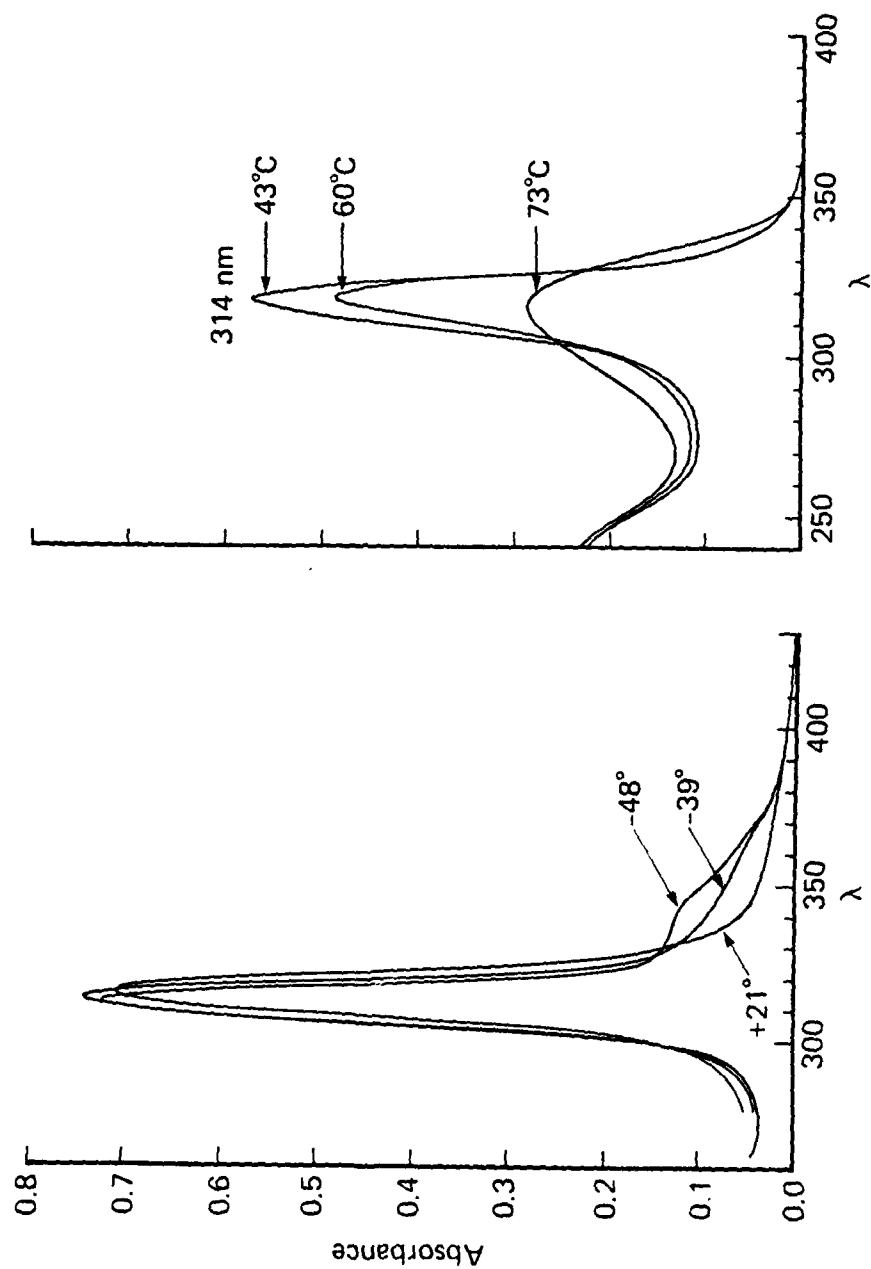
Figure 2. Variable temperature UV spectra of a poly(di-n-pentylsilane) (PDPS) film.
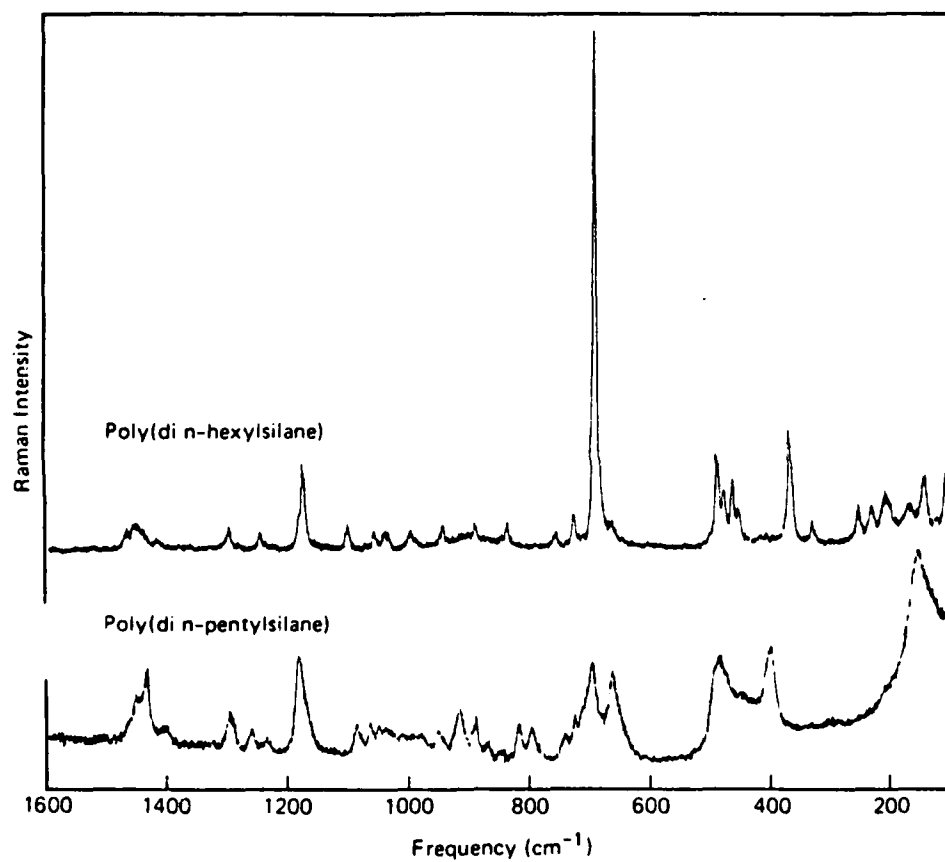
Figure 3. Raman spectra of PDHS (upper) and PDPS (lower) at 21°C.

²⁹Si CPMAS NMR

Figure 4. Variable tempreature CPMAS ²⁹Si NMR spectra of PDHS (left) and PDPS (right).

Figure 5. Room temperature, wide angle x-ray diffraction (WAXD) pictures of stretch oriented samples of PDHS (upper) and PDPS (lower).

Figure 6. Projection of the 7/3 helical conformation of PDPS onto a plane normal to the helical axis. Silicon atoms are represented by the larger filled circles, carbon atoms by the smaller.

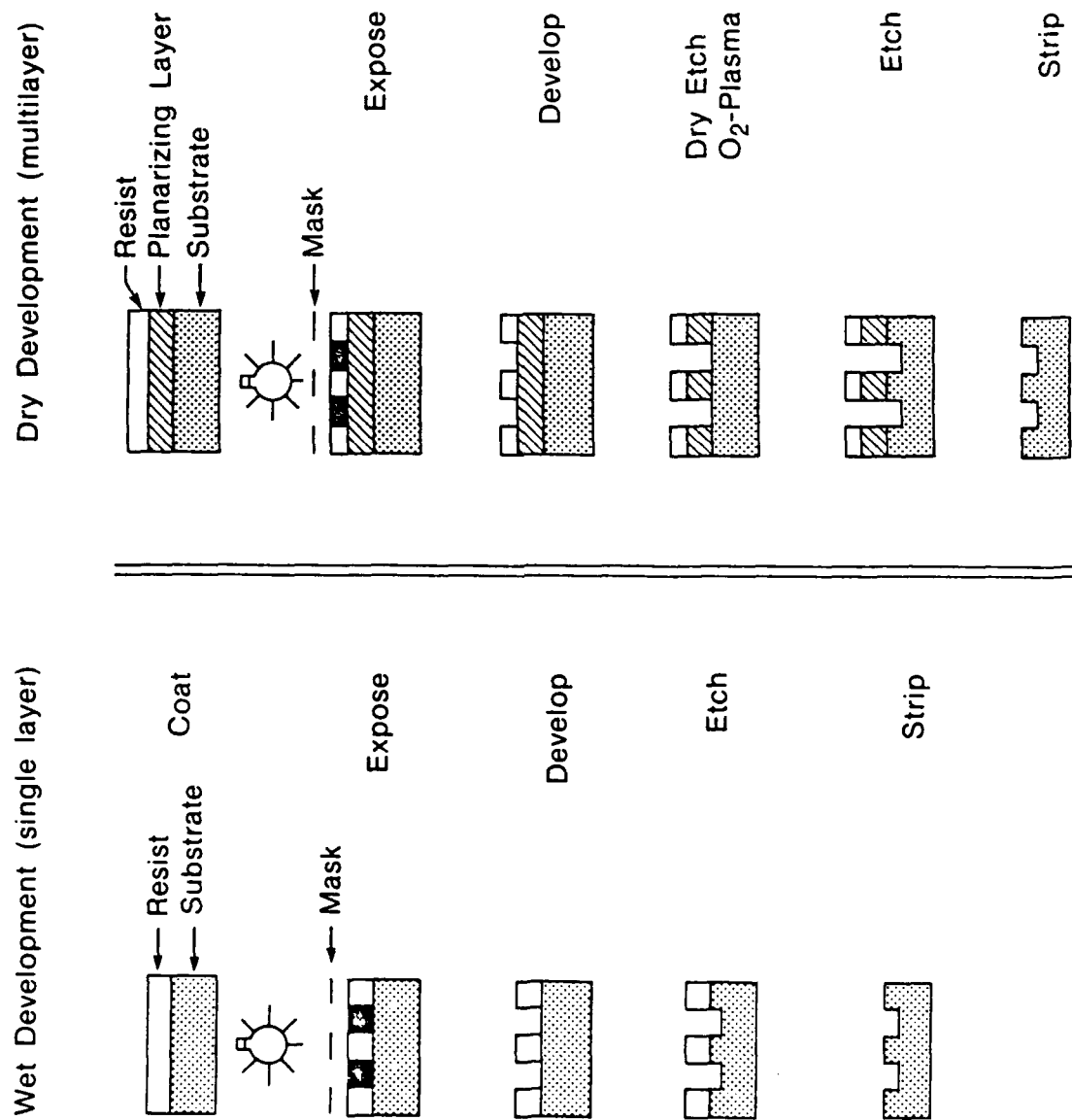Figure 7. The photochemical bleaching of poly(hexylmethylsilane) at 313 nm.

Wet Development (single layer)

Coat
— Resist
— Substrate

— Mask

Expose

Develop

Etch

Strip

Dry Development (multilayer)

— Resist
— Planarizing Layer
— Substrate

— Mask

Expose

Develop

Dry Etch
O_2-Plasma

Etch

Strip

Figure 8. A schematic for a typical single layer (left) and a multilayer lithographic process.

Figure 9. 0.75 μm features produced in a bilyer composed of 0.2 μm poly(methyl-cyclohexylsilane) coated over 2.0 μm of a hardbaked Novolac-naphthoquinone-2-diazide photoresist; mid-UV projection lithography, 100 mJ/cm^2, O$_2$-RIE image transfer.
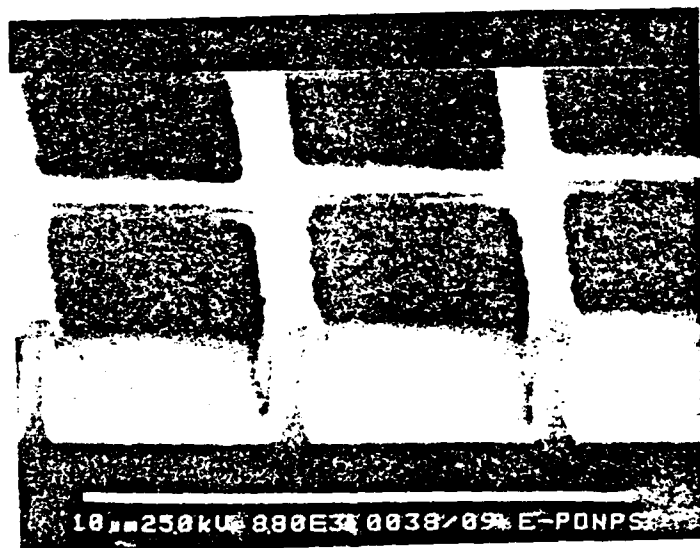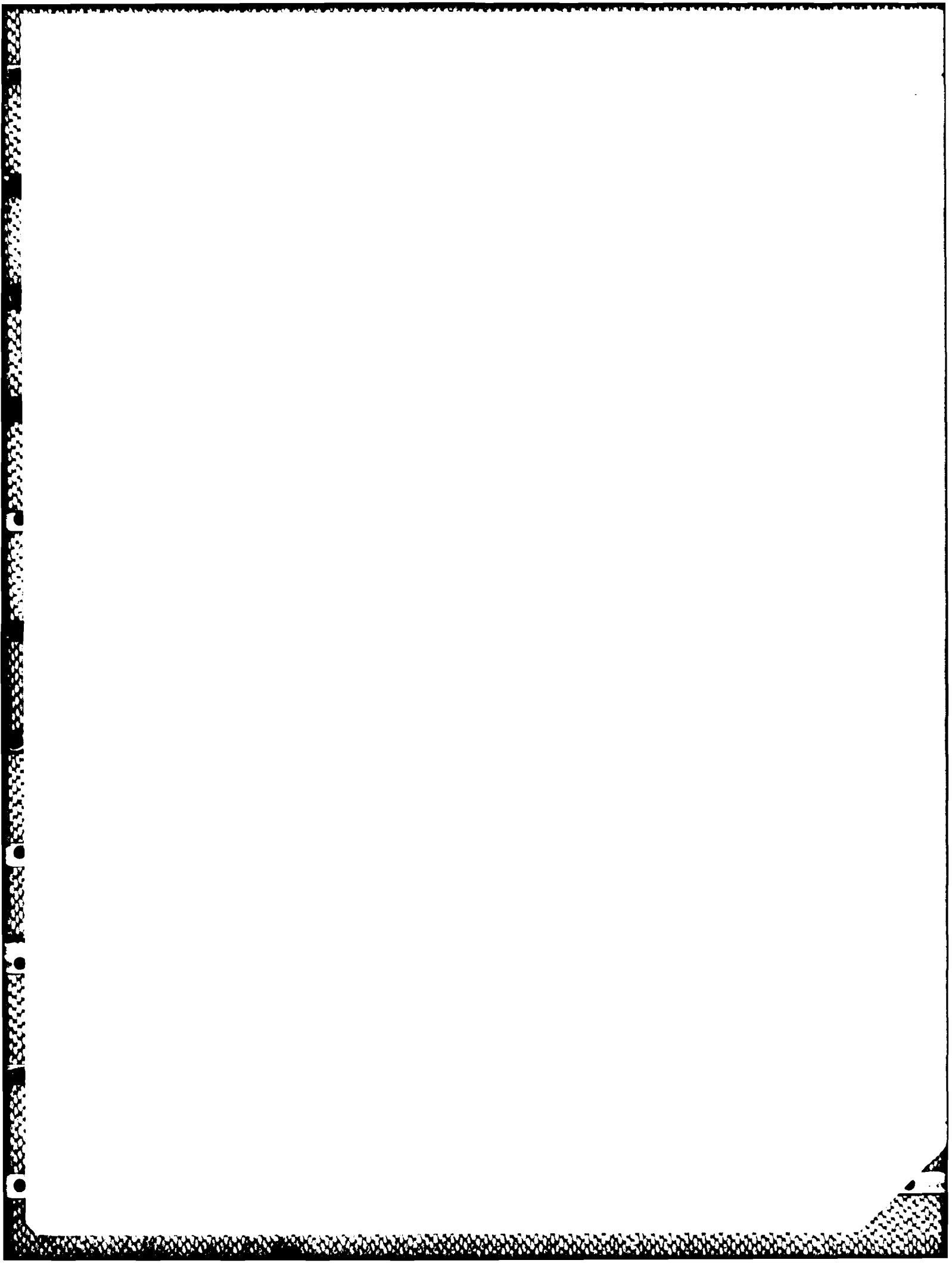
Figure 10. Submicron features generated by e-beam imaging of 0.14 μm of an aliphatic polysilane over 2.0 μm of hardbaked Novolac-naphthoquinone-2-diazide photoresist; 20 μC, O_2-RIE image transfer.

END

Feb.

1988

DTIC